文章编号:1006-9941(2022)07-0694-09

Effect of DAAzF on the Thermal Performance of DAAF

ZHUANG Si-qi[1], **FU Xiao-lin**[1], **YU Qian**[2], **CHEN Jian-bo**[2], **LIU Yu**[2], **JIN Bo**[1], **HUANG Hui**[1,2]

(1. *School of Materials Science and Engineering, Southwest University of Science and Technology, Mianyang* 621010, *China*; 2. *Institute of Chemical Materials, China Academy of Engineering Physics, Mianyang* 621999, *China*)

Abstract: 3,3′-Diamino-4,4′-azofurazan (DAAzF) is one of the main impurities that produced during the synthesis of 3,3′-diamino-4,4′-azoxyfurazan (DAAF). However, the effect of DAAzF on the thermal performance of DAAF remains unclear in the past. To this end, a doping strategy based on the dissolution-precipitation method was developed to prepare DAAF@DAAzF explosives by uniformly doping 0.5%−10% DAAzF into DAAF, and the effect of DAAzF on the thermal performance of DAAF@DAAzF explosives was investigated by using simultaneous thermogravimetry and differential scanning calorimetry. The doping of DAAzF decreases the melting point of DAAF-based explosives, with the greatest decrease from 246.4 ℃ to 239.3 ℃ occurring at 10% DAAzF content. For the first time, it is found that the eutectic mixture can be formed when the mass ratio of DAAzF/DAAF is 5/95. Further, the presence of DAAzF decreases the activation energies and pre-exponential factors of DAAF-based explosives during the initial decomposition. Therefore, DAAzF as an impurity accelerates the thermal decomposition of DAAF@DAAzF explosives and reduces their thermal stability.

Key words: 3, 3′-diamino-4, 4′-azoxyfurazan (DAAF); 3, 3′-diamino-4, 4′-azofurazan (DAAzF); thermal performance; DAAF@DAAzF explosives; the impurity

CLC number: TJ55; O64 **Document code**: A **DOI**: 10.11943/CJEM2022022

1 Introduction

Insensitive energetic materials based on furazan rings have received wide attention in the last decade due to their favorable properties including high energy density, good safety, and high nitrogen content[1−3]. Among them, 3,3′-diamino-4,4′-azoxyfurazan (DAAF) is regarded as one of the most promising explosives due to its good thermal stability, high positive enthalpy, high detonation velocity of 8.02 km·s^{-1}, and detonation pressure of 30.6 GPa[4−5]. DAAF, as an excellent explosive, is expected to be used in place of 1,3,5-triamino-2,4,6-trinitrobenzene (TATB) in insensitive booster explosives and hexahydro-1,3,5-trinitro-1,3,5-triazine (RDX) in melt cast explosives[6−7]. However, it is reported that the impurities have a negative effect on the thermal performance of DAAF, as the onset temperature of DAAF measured by differential scanning calorimetry (DSC) is decreased from 250 ℃ to 128 ℃ by the impurities [8]. Therefore, it is necessary to study the change of DAAF's thermal performance in the presence of the impurities.

For the preparation of nano-explosives and plastic-bonded explosives[7, 9], DAAF is mainly synthesized based on the Oxone oxidation method[8], which yields as well various impurities such as unreacted precursors, intermediates, and side-products. In our previous study, we found that the impurities of DAAF could not be ignored with a relatively high content of 6.62% of DAAF final product[10]. It is very

Received Date: 2022-01-24; **Revised Date**: 2022-02-26

Published Online: 2022-05-26

Project Supported: National Natural Science Foundation of China (No. 21975235)

Biography: ZHUANG Si-qi(1996−), female, master, research field: the analysis of energetic materials. e-mail: siqizhuang@163.com

Corresponding author: HUANG Hui(1961−), male, professor, research field: the preparation of energetic materials. e-mail: huanghui@caep.cn

CHEN Jian-bo(1985−), male, associate professor, research field: the analysis of energetic materials. e-mail: chenjianbo@caep.cn

引用本文:庄思琪,付小林,于谦,等. DAAzF对DAAF热性能的影响[J]. 含能材料,2022,30(7):694−702.

ZHUANG Si-qi, FU Xiao-lin, YU Qian, et al. Effect of DAAzF on the Thermal Performance of DAAF[J]. *Chinese Journal of Energetic Materials (Hanneng Cailiao)*, 2022, 30(7):694−702.

difficult to remove 3, 3′-diamino-4, 4′-azofurazan (DAAzF) from DAAF via common purification due to the similar structure between DAAzF and DAAF. Compared to DAAF, DAAzF only lacks an oxygen atom that bound to the azo group. Therefore, DAAzF is regarded as a major impurity of DAAF[11-12]. Some properties of DAAzF itself have been investigated in the past. The vacuum thermal stability test of DAAzF is 5.87 $mL \cdot g^{-1}$, which is much higher than that of DAAF (0.69 $mL \cdot g^{-1}$)[13-15]. Besides, the detonation velocity and pressure of DAAzF are 7.42 $km \cdot s^{-1}$ and 26.2 GPa, respectively, which are lower than that of DAAF[16]. However, there is no study about the effect of DAAzF as the co-existing impurity on the thermal performance of DAAF until now.

In this study, we investigated the effect of DAAzF on the thermal performance of DAAF for the first time. DAAzF was firstly synthesized, and then several composite DAAF@DAAzF explosives were obtained by doping different content of DAAzF into DAAF. Subsequently, the doping process of DAAF@DAAzF explosives was investigated by analyzing the DAAzF content and the characterizing the morphology. Further, the thermal performances of DAAF@DAAzF explosives, including melting point, thermal decomposition temperature, and activation energy, were investigated via simultaneous thermogravimetry and differential scanning calorimetry (TG-DSC). In addition, the thermal stability of DAAF explosives in the presence of DAAzF was obtained through the study of isothermal thermal decomposition.

2 Experimental Section

2.1 Reagents and instrumentations

3,4-Diaminofurazan(DAF), DAAF and DAAzF were synthesized in our laboratory. Analytical reagent(AR) *N*,*N*-dimethylformamide(DMF) was purchased from Kelong Chemical (Chengdu, Sichuan).

High-performance liquid chromatography (HPLC) grade acetonitrile was purchased from Merck Chemicals (Darmstadt, Germany). Ultrapure water was purified by a Millipore-Q system (Bedford, USA) with the resistivity of 18.2 MΩ. Thermal analysis was performed on Mettler Toledo TG-DSC 3+ (Zurich, Switzerland). Chromatography analysis was carried out with an Agilent 1260 infinity ultrahigh-performance liquid chromatography (HPLC) system (Waldbronn, Germany). Powder X-Ray diffraction(PXRD) was measured on a Bruker D8 Advance diffractometer (Karlsruhe, Germany). Scanning electron microscopy(SEM) was conducted on a Zeiss high-resolution field emission scanning electron microscopy instrument (Oberkochen, Germany).

2.2 Sample preparation

DAF, DAAF and DAAzF were synthesized according to the reported literature[17].

DAAF (10 g) and different weights of DAAzF (0-1.0 g) were added into DMF (10 mL), and then the mixture was stirred at 60 ℃. After complete dissolution, cool water was added quickly into the above solution, and then the precipitates were filtered, washed, and dried to obtain DAAF@DAAzF explosives. The composite explosives doped with 0.5%, 1.0%, 2.5%, 5.0%, and 10% mass fractions were named as DAAF@DAAzF-1, DAAF@DAAzF-2, DAAF@DAAzF-3, DAAF@DAAzF-4, and DAAF@DAAzF-5, respectively. As a control experiment, raw DAAF without the addition of DAAzF was performed by the above method.

2.3 The characterization of DAAF@DAAzF

DAAF@DAAzF explosives were measured by PXRD. The tube current and voltage of PXRD were set at 40 mA and 40 kV, respectively, and the images were scanned in a range of 2θ from 10° to 40° by using a Vantec detector with Cu Kα as radiation (λ = 1.54180 Å). Meanwhile, the morphology and particle size of DAAF@DAAzF were characterized by SEM.

The solution of DAAF@DAAzF explosives was prepared with the concentration of 1.0 $mg \cdot mL^{-1}$ in acetonitrile and then diluted to the concentration of 1.0 $\mu g \cdot mL^{-1}$ for chromatographic analysis. The

above solution was filtered through a 0.45 μm membrane before the HPLC analysis. Then, the diluted solution of DAAF@DAAzF explosives was analyzed by HPLC with reversed-phase Hypersil Gold C_{18} column (100 mm×2.1 mm, 1.9 μm). The mobile phase consisted of acetonitrile and ultrapure water. The flow rate was set at 0.5 mL·min^{-1}. The temperature of HPLC column oven was set at 35 ℃. The detection wavelength of HPLC was set at 230 nm.

2.4 Thermal analysis of raw DAAF and DAAF@DAAzF explosives

Thermal analysis of both raw DAAF and DAAF@DAAzF explosives were performed by TG-DSC. All the experiments were measured in encapsulated aluminum pans with a low-sized pinhole. The mass of all explosives was about 1.5 mg for each measurement. Nitrogen was chosen as the shield gas with a flow rate of 30 mL·min^{-1}. For the programmed heating measurements, all explosives were heated from 30 ℃ to 350 ℃ under different heating rates of 2, 5, 10 K·min^{-1} and 20 K·min^{-1}, respectively. All data of thermal analysis was processed by using the Netzsch kinetics Neo Trial software[18].

3 Results and Discussion

3.1 The doping of DAAzF in DAAF

It would be more homogeneous to dope DAAzF in DAAF through the dissolution-precipitation method compared to the direct mixing of two different solid powders, because all molecules of DAAF and DAAzF can be homogeneously dispersed in the same solvent (DMF) before the precipitation. With that in mind, DAAF explosives were doped with different mass fractions of DAAzF from 0.5% to 10% to prepare DAAF@DAAzF explosives via the dissolution-precipitation method, which is shown in Fig.1.

3.2 The analysis of DAAzF content

PXRD was used to characterize the doping of DAAzF in DAAF@DAAzF explosives. PXRD patterns of raw DAAF and DAAF@DAAzF explosives are shown in Fig. 2a. It is shown that the signal of raw DAAF at 27.70° disappears after doping 0.5% DAAzF.

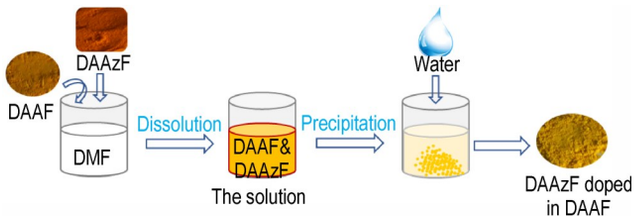

Fig.1 The process of doping DAAzF into DAAF

When 10% DAAzF is doped in DAAF@DAAzF explosives, two signals of DAAzF at 20.08° and 28.02° are observed obviously, which indicates that DAAF@DAAzF explosives contain DAAzF. To obtain the quantitative analysis of the doping content of DAAzF, the content of DAAzF in DAAF@DAAzF explosives was further analyzed by HPLC in Fig. 2b. Chromatographic peaks of DAAF and DAAzF are separated fully by HPLC, because DAAF and DAAzF have different retention times of 8.70 min and 9.36 min, respectively. Although raw DAAF has a very weak signal of DAAzF due to raw DAAF itself containing tiny DAAzF as a byproduct before the doping (Table 1), the signals of DAAzF in DAAF@DAAzF explosives become stronger gradually with the increase of DAAzF content. After the deduction of background signal of DAAzF in raw DAAF, DAAF@DAAzF explosives including DAAF@DAAzF-1, DAAF@DAAzF-2, DAAF@DAAzF-3, DAAF@DAAzF-4, DAAF@DAAzF-5 were doped with 0.5%, 1.0%, 2.5%, 5.0%, and 10% DAAzF, respectively. Moreover, the SEM images in Fig.2c show the morphology of DAAF@DAAzF explosives is more homogeneous compared to raw DAAF, and the particle size of DAAF@DAAzF explosives is less than 1.0 μm. Therefore, different contents of DAAzF are homogeneously doped in DAAF@DAAzF explosives.

3.3 Mass loss

All TG/DTG curves of raw DAAF and DAAF@DAAzF explosives were determined by TG-DSC with the heating rate at 10 K·min^{-1}. According to the TG curves of Fig. 3a, DAAF@DAAzF explosives display a mass loss in one step for their thermal decomposition. The mass loss begins at about 244.3 ℃, and then there is about 60% mass loss observed after 10 min. Through the analysis of DTG

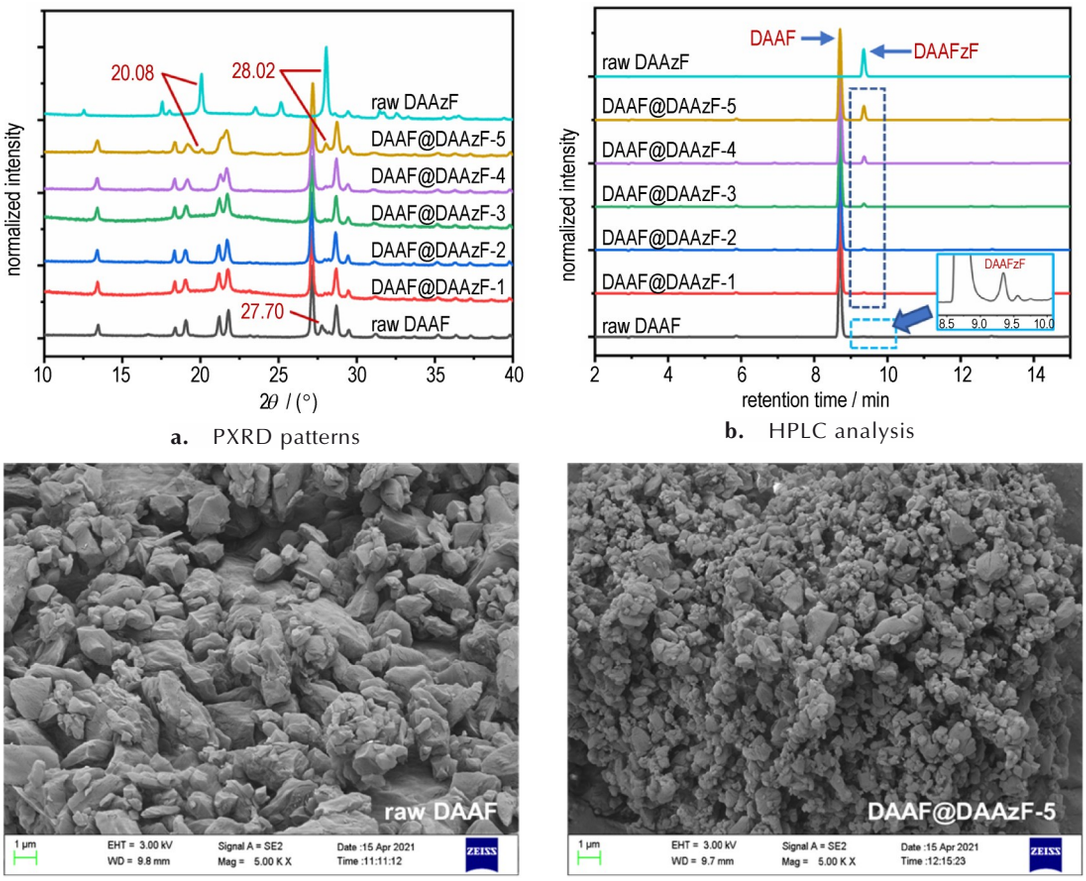

a. PXRD patterns **b.** HPLC analysis

c. SEM images

Fig.2 PXRD, HPLC and SEM analysis of raw DAAF, raw DAAzF and DAAF@DAAzF explosives

Table 1 HPLC data of different content of DAAzF doped in DAAF@DAAzF explosives

samples	retention time of DAAF / min	retention time of DAAzF / min	total content of DAAzF / %	background content / %	doping content of DAAzF / %
raw DAAF	8.70	9.36	0.16	0.16	0
DAAF@DAAzF-1	8.70	9.36	0.68	0.18	0.5
DAAF@DAAzF-2	8.70	9.36	1.15	0.15	1.0
DAAF@DAAzF-3	8.71	9.36	2.59	0.09	2.5
DAAF@DAAzF-4	8.70	9.36	5.11	0.11	5.0
DAAF@DAAzF-5	8.70	9.36	10.13	0.13	10

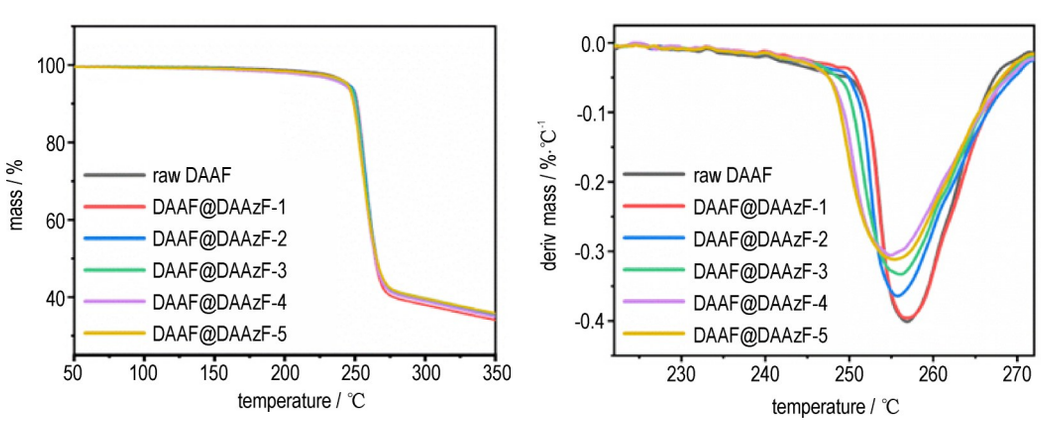

a. TG curves **b.** DTG curves

Fig.3 TG and DTG curves of raw DAAF and DAAF@DAAzF explosives at 10 K·min^{-1}

curves in Fig.3b, an obvious difference is found between raw DAAF and DAAF@DAAzF explosives. The peak temperature in the DTG curve is 256.7 ℃ for raw DAAF. The DTG peak temperature of DAAF@DAAzF explosives decreases with the increase of DAAzF content. The peak temperature is 255.8 ℃ for DAAF@DAAzF-2 with 1.0% DAAzF, and 254.8 ℃ for DAAF@DAAzF-4 with 5.0% DAAzF. Meanwhile, the mass loss rate of DAAF@DAAzF explosives increases with the increase of DAAzF content at the initial stage of thermal decomposition. However, the mass loss rate becomes slow under higher content of DAAzF doped in DAAF@DAAzF explosives at the end of thermal decomposition. Therefore, the doping of DAAzF can slightly lower the peak temperature of DAAF-based explosives in DTG curves.

3.4 Melting point and melting heat

The DSC curves of DAAF@DAAzF explosives were investigated under the heating rate of 10 K·min^{-1} in Fig. 4a. An endothermic peak of raw DAAF is observed at 249.0 ℃, which indicates there is an endothermic process before thermal decomposition. Through the endothermic reaction, DAAF melts to provide a liquid phase for its thermal decomposition, which is similar to RDX and HMX[15, 19-20]. Meanwhile, melting point of DAAF@DAAzF explosives decreases with increasing DAAzF content, which is shown in Fig. 4b. The melting point of raw DAAF is 246.4 ℃. At the heating rate of 10 K·min^{-1}, melting points of DAAF@DAAzF explosives with 0.5%, 1.0%, 2.5%, 5.0%, and 10% DAAzF are 245.9, 245.1, 244.4, 242.9 ℃, and 239.3 ℃, respectively, which indicates that DAAzF as the impurity obviously decreases the melting point of DAAF-based explo-

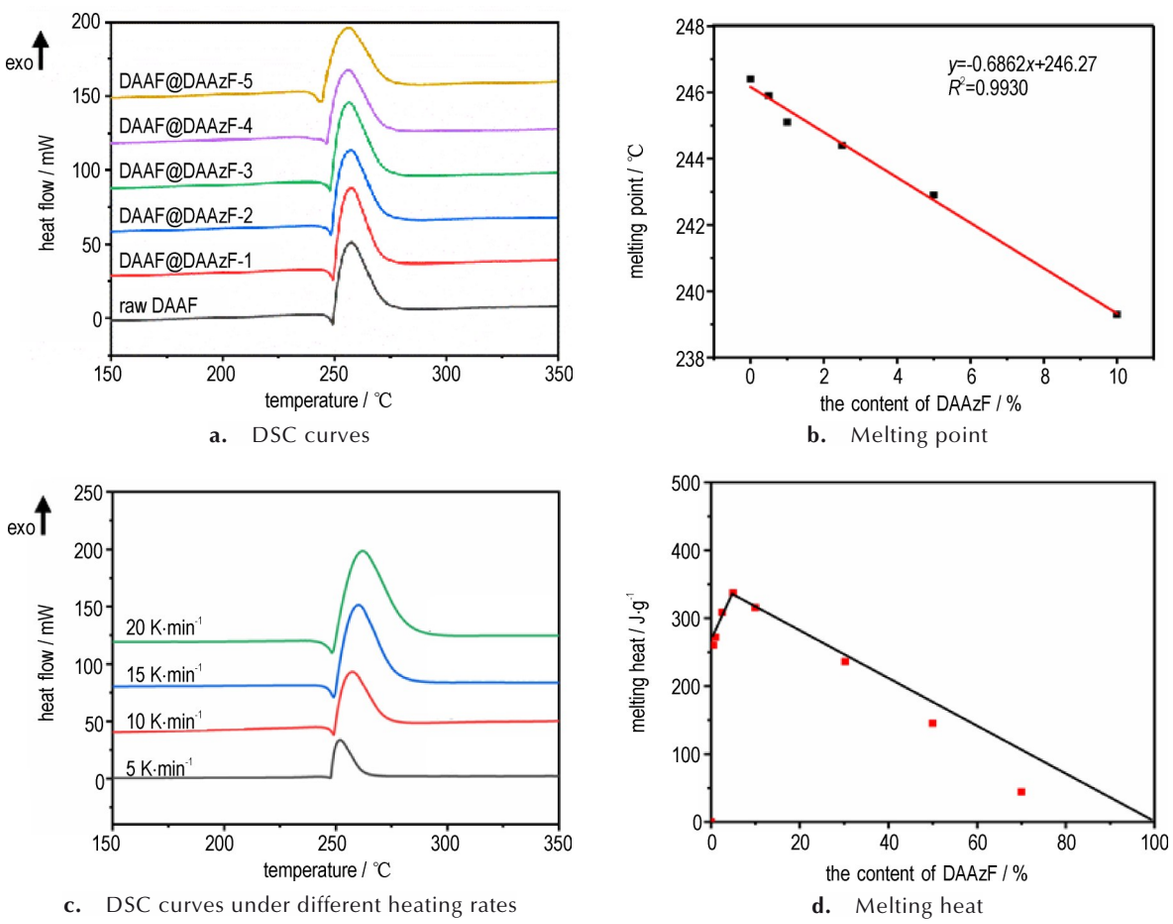

a. DSC curves **b.** Melting point

c. DSC curves under different heating rates **d.** Melting heat

Fig.4 DSC curves and melting points of raw DAAF and DAAF@DAAzF explosives at 10 K·min^{-1}, DSC curves of raw DAAF under different heating rates, and melting heat of raw DAAF and DAAF@DAAzF explosives at 20 K·min^{-1}

sives. A linear relationship (y=−0.6862x+246.27) is found between the melting point of DAAF@DAAzF explosives (y) and the content of DAAzF (x) with an R^2 value of 0.9930, which is in agreement with Raoult's law of colligative property in dilute solution[21]. Compared to solid-phase decomposition, DAAF@DAAzF explosives display much faster thermal decomposition at the initial melting stage due to the decrease of melting points by DAAzF, which is in good agreement with the change of mass loss of DAAF@DAAzF explosives.

Further, the DSC curves of raw DAAF were measured under different heating rates in Fig.4c. The melting heat of raw DAAF under 5, 10, 15 K·min^{-1}, and 20 K·min^{-1} is 211.09, 184.34, 146.93 J·g^{-1}, and 125.59 J·g^{-1}, respectively. Normally, the melting point of raw DAAF keeps constant under different heating rates. However, the decomposition temperature of raw DAAF at a higher heating rate of 20 K·min^{-1} apparently lags behind that at a low heating rate of 5 K·min^{-1}. So, the melting heat of raw DAAF decreases with the increase of the heating rate. As shown in Fig. 4d, the melting heat of DAAF@DAAzF explosives after the doping of DAAzF was also investigated at 20 K·min^{-1}. The melting heat of DAAF@DAAzF explosives increases with the increase of DAAzF content, when the doping content of DAAzF is less than 5.0%. DAAF@DAAzF-4 containing 5.0% DAAzF displays the maximum melting heat with the value of 337.38 J·g^{-1}. The melting heat of DAAF@DAAzF explosives decreases with the increase of DAAzF content, when DAAzF content is higher than 5.0%. Therefore, the change of melting heat indicates the eutectic mixture is formed between 5.0% DAAzF and 95% DAAF.

Besides, the melting process of DAAF@DAAzF-3 containing 2.5% DAAzF is successfully observed by a microscopic melting point meter in Fig. 5. During the melting process, solid samples began to spin and move, and then melted with the bubbles appearing, which indicates that thermal decomposition of DAAF@DAAzF explosives includes solid decomposition, melting, and liquid decomposition. Thus, it is further demonstrated that the thermal process of DAAF-based explosives containing DAAzF includes both melting and thermal decomposition.

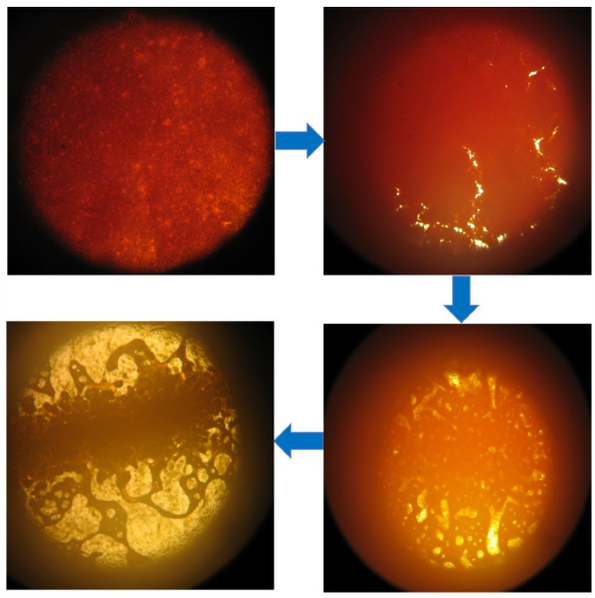

Fig.5 The melting process of DAAF@DAAzF-3 containing 2.5% DAAzF

3.5 Kinetic analysis

Kinetic parameters of thermal decomposition of DAAF explosives in the presence of DAAzF were calculated by Friedman method (Eq. (1)) based on TG curves at different heating rates[20]:

$$\ln\left(\beta_i\left(\frac{\mathrm{d}\alpha}{\mathrm{d}T}\right)\alpha, i\right) = \ln\left[f(\alpha)A_\alpha\right] - \left(\frac{E_a}{RT_{\alpha,i}}\right) \quad (1)$$

where E_a is the apparent activation energy, kJ·mol^{-1}; A is the pre-exponential (frequency) factor, s^{-1}; α is the conversion fraction; β is the heating rate, K·min^{-1}; R is the gas constant, 8.314 J·mol^{-1}·K^{-1}; T is the absolute temperature, K; $f(\alpha)$ is the differential expression of the reaction model function. The pre-exponential factor (A) can be found by model-free analysis only assumption of known function $f(\alpha)$, which is often used in the view of reaction of n^{th} order in model-free analysis.

As shown in Fig. 6a, a high activation energy ((560.9±60.8) kJ·mol^{-1}) of raw DAAF is obtained at the initial thermal decomposition (α <0.30), which may be attributed to several coexisting processes of solid decomposition: melting and liquid

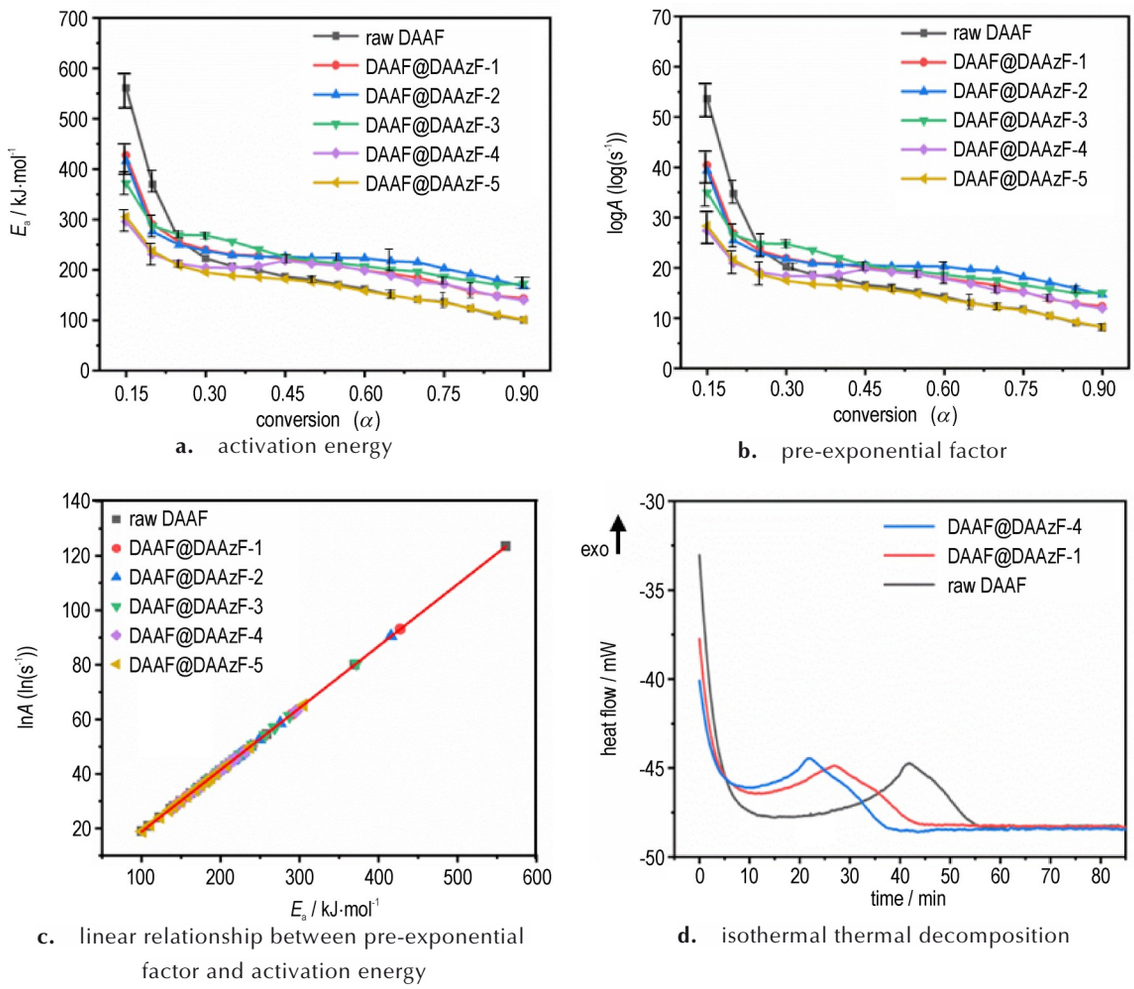

Fig. 6 Activation energies and pre-exponential factors of raw DAAF and DAAF@DAAzF explosives under different conversion (α), linear relationship between pre-exponential factor (ln(A)) and activation energy (E_a), and isothermal thermal decomposition of raw DAAF and DAAF@DAAzF explosives

decomposition. The doping of DAAzF can decrease the activation energy of DAAF-based explosives, which is similar to the decrease of melting point and mass loss rate of DAAF@DAAzF explosives. After doping with 0.5% DAAzF, the activation energy of DAAF@DAAzF-1 is decreased to (423.2±6.9) kJ·mol^{-1}. The activation energy decreases as the reaction goes on. The change of activation energy of DAAF@DAAzF explosives becomes slow when the conversion is over 0.30. The activation energy values of all DAAF@DAAzF explosives range from (155.3±9.9) kJ·mol^{-1} to (213.2±44.2) kJ·mol^{-1} under high conversion ($\alpha \geqslant 0.30$), which is in agreement with that of the reported DAAF explosive[4, 16]. As shown in Fig. 6b, pre-exponential factors (log$A$) of all DAAF-based explosives show similar trends with their activation energies. Before the doping of DAAzF, raw DAAF shows a high pre-exponential factor with log$A$ of (39.3±3.3) s^{-1}. However, the pre-exponential factor of DAAF@DAAzF explosives is decreased with log$A$ ranging from (31.7±1.3) s^{-1} to (23.4±1.5) s^{-1} during the initial decomposition when the doping content of DAAzF is over 0.5%.

Further, there is a kinetic compensation effect existing between apparent activation energy and pre-exponential factor, which means a linear relationship (ln$A$=a+bE_a) between ln$A$ and E_a[22-23]. As shown in Fig. 6c and Table 2, different content of DAAzF shows nearly the same slopes of 0.227~0.229 by performing a plot of ln$A$ against E_a with a good linear relationship of R^2=0.9999, which indicates raw DAAF and DAAF@DAAzF explosives have

the same decomposition mechanism. According to Eq. (2)[24], the decomposition rate constant (k) of raw DAAF is (1.11×10^{-3}) s^{-1} at 250 ℃. After the doping of DAAzF, the rate constant of thermal decomposition increases with the increase of DAAzF content, and the k value of DAAF@DAAzF-5 containing 10% DAAzF is (3.59×10^{-3}) s^{-1}:

$$\frac{d\alpha}{dt} = k(T)f(\alpha) \quad (2)$$

where $d\alpha/dt$ is the reaction rate, s^{-1}; α is the conversion fraction; $k(T)$ is the rate constant, s^{-1}; t is time, s; T is temperature, K; $f(\alpha)$ is the reaction model.

In addition, the isothermal thermal decomposition of DAAF@DAAzF explosives was investigated before the melting. Fig. 6d displays the isothermal DSC curves of all DAAF-based explosives at 230 ℃. It can be found that the decomposition peak time of raw DAAF is located at 41.72 min. After doping with 0.5% and 5.0% DAAzF, the DSC peak time of DAAF@DAAzF-1 and DAAF@DAAzF-4 is decreased to 27.09 min and 21.75 min, respectively. Compared to raw DAAF, isothermal thermal decomposition of DAAF@DAAzF explosives occurs in advance due to the doping of DAAzF. Therefore, the doping of DAAzF decreases the thermal stability of DAAF-based explosives.

Table 2 The parameters of linear equations between pre-exponential factors and activation energies

samples	$\ln A=a+bE_a$	R^2	k / s^{-1}
raw DAAF	$\ln A=0.227E_a-3.917$	0.9999	1.11×10^{-3}
DAAF@DAAzF-1	$\ln A=0.227E_a-4.024$	0.9999	1.22×10^{-3}
DAAF@DAAzF-2	$\ln A=0.228E_a-4.277$	0.9999	1.31×10^{-3}
DAAF@DAAzF-3	$\ln A=0.229E_a-4.530$	0.9999	1.66×10^{-3}
DAAF@DAAzF-4	$\ln A=0.228E_a-4.301$	0.9999	2.74×10^{-3}
DAAF@DAAzF-5	$\ln A=0.227E_a-4.028$	0.9999	3.59×10^{-3}

4 Conclusions

(1) The effect of DAAzF on the thermal performance of DAAF@DAAzF explosives were studied comprehensively by TG-DSC after doping different content of DAAzF from 0.5% to 10% in DAAF explosives.

(2) DAAzF decreases the melting points of DAAF@DAAzF explosives, with the largest decline of 7.1 ℃ in the presence of 10% DAAzF. The doping of 5.0% DAAzF in DAAF can lead to the formation of the eutectic mixture between them.

(3) The coexistence of DAAzF also decreases the activation energies and pre-exponential factors of DAAF@DAAzF explosives during the initial decomposition. Meanwhile, DAAzF can increase the rate constant of thermal decomposition of DAAF-based explosives.

(4) Through isothermal thermal decomposition, the decomposition peak time of DAAF@DAAzF explosives is advanced clearly due to the presence of DAAzF. Therefore, DAAzF as an impurity accelerates the thermal decomposition of DAAF-based explosives and decreases their thermal stability.

Acknowledgements: This work was financially supported by the National Natural Science Foundation of China (No. 21975235).

References:

[1] LIU Yu-ji, ZHANG Jia-heng, WANG Kang-cai, et al. Bis(4-nitraminofurazanyl-3-azoxy) azofurazan and derivatives: 1, 2, 5-oxadiazole structures and high-performance energetic materials[J]. *Angewandte Chemie*, 2016, 55(38): 11548-11551.

[2] TALAWAR M B, SIVABALAN R, SENTHIKUMAR N, et al. Synthesis, characterization and thermal studies on furazan- and tetrazine-based high energy materials[J]. *Journal of Hazardous Materials*, 2004, 113(1): 11-25.

[3] ZHANG Jia-heng, SHREEVE J M. 3, 3′-Dinitroamino-4, 4′-azoxyfurazan and its derivatives: An assembly of diverse N—O building blocks for high-performance energetic materials[J]. *Journal of the American Chemical Society*, 2014, 136(11): 4437-4445.

[4] KOCH E C. Insensitive high explosives II: 3, 3′-diamino-4, 4′-azoxyfurazan (DAAF)[J]. *Propellants, Explosives, Pyrotechnics*, 2016, 41(3): 526-538.

[5] CHELLAPPA R S, DATTELBAUM D M, COE J D, et al. Intermolecular stabilization of 3, 3′-diamino-4, 4′-azoxyfurazan (DAAF) compressed to 20 GPa[J]. *Journal of Physical Chemistry A*, 2014, 118(31): 5969-5982.

[6] BADUJAR D M, TALAWAR M B. Thermokinetic decomposition and sensitivity studies of 4, 4′-diamino-3, 3′-azoxy furazan (DAAF)-based melt cast explosive formulations[J]. *Journal of Energetic Materials*, 2018, 36(3): 316-324.

[7] CHIQUETE C, JACKON S I, ANDERSON E K, et al. Detonation performance experiments and modeling for the DAAF-based high explosive PBX 9701[J]. *Combustion and Flame*, 2021(223): 382-397.

[8] FRANCOIS E G, CHAVEZ D E, SANDSTROM M M. The development of a new synthesis process for 3, 3′-Diamino-4, 4′-azoxyfurazan (DAAF)[J]. *Propellants, Explosives, Pyrotechnics*, 2010, 35(6): 529−534.
[9] WANG Jun, QU Yan-yang, WANG Yao, et al. Preparation of nano-DAAF explosive with improved initiation sensitivity[J]. *Propellants, Explosives, Pyrotechnics*, 2018, 43(10): 1060−1064.
[10] CHEN Jian-bo, DING Huan, LI Jian-jun, et al. Development and validation of HPLC method for DAAF and its applications in quality control and environmental monitoring[J]. *Propellants, Explosives, Pyrotechnics*, 2020, 45(10): 1580−1589.
[11] CHAVEZ D, HILL L, HISKEY M, et al. Preparation and explosive properties of azo-and azoxy-furazans[J]. *Journal of Energetic Materials*, 2000, 18(2−3): 219−236.
[12] WANG Luo-xin, TUO Xin-lin, YI Chang-hai, et al. Theoretical study on the trans-cis isomerization and initial decomposition of energetic azofurazan and azoxyfurazan[J]. *Journal of Molecular Graphics and Modelling*, 2009, 28(2): 81−87.
[13] CANNIZZO L F, HAMILTON R S, HIGHSMITH T K, et al. Furazan-based energetic ingredients[R]. Thiokol Propulsin Brigham City UT, 1999.
[14] SINDISKII V P, VU M C, SHEREMETEV A B, et al. Study on thermal decomposition and combustion of insensitive explosive 3,3′-diamino-4,4′-azofurazan (DAAzF)[J]. *Thermochimica Acta*, 2008, 473(1−2): 25−31.
[15] LI Ji-zhen, WANG Bo-zhou, FAN Xue-zhong, et al. Interaction and compatibility between DAAzF and some energetic materials[J]. *Defence Technology*, 2013, 9(3): 153−156.
[16] LI Hong-zhen, HUANG Ming, ZHOU Jian-hua, et al. Properties of diaminoazofurazan and diaminoazoxyfurazan[J]. *Chinese Journal of Energetic Materials*, 2006, 14(5): 381−384.
[17] GAO Li, YANG Hong-wei, TANG Yong-xing, et al. Synthesis and characterization of azofurazan and azoxyfurazan[J]. *Chinese Journal of Explosives & Propellants*, 2013,36(1): 47−51.
[18] SESTAK J. Thermal analysis and thermodynamic properties of solids[M]. Amsterdam: Elsevier, 2021.
[19] SINAPOUR H, DAMIRI S, POURETEDAL H R. The study of RDX impurity and wax effects on the thermal decomposition kinetics of HMX explosive using DSC/TG and accelerated aging methods[J]. *Journal of Thermal Analysis and Calorimetry*, 2017, 129(1): 271−279.
[20] SINAPOUR H, DAMIRI S, RAVANBOD M, et al. The effect of HMX impurity and irganox antioxidant on thermal decomposition kinetics of RDX by TG/DSC non-isothermal method[J]. *Propellants, Explosives, Pyrotechnics*, 2019, 44(4): 429−437.
[21] HILDEBRAND J H. A quantitative treatment of deviations from Raoult's Law[J]. *Proceedings of the National Academy of Sciences of the United States of America*, 1927, 13(5): 267−272.
[22] BRILL T, GONGWER P, WILLIAMS G K. Thermal decomposition of energetic materials. 66. Kinetic compensation effects in HMX, RDX, and NTO[J]. *Journal of Physical Chemistry*, 1994, 98(47): 12242−12247.
[23] LIU Zi-ru, LIU Yan, FAN Xi-ping, et al. Thermal decomposition of RDX and HMX explosives part III: Mechanism of thermal decomposition[J]. *Chinese Journal of Explosives & Propellants*, 2006, 29(4): 14−18.
[24] SILVA J, ALARCON R T, GAGLIERI C, et al. New thermal study of polymerization and degradation kinetics of methylene diphenyl diisocyanate[J]. *Journal of Thermal Analysis and Calorimetry*, 2018, 133(3): 1455−1462.

DAAzF对DAAF热性能的影响

庄思琪[1],付小林[1],于 谦[2],陈建波[2],刘 渝[2],金 波[1],黄 辉[1,2]
(1. 西南科技大学材料科学与工程学院, 四川 绵阳 621010; 2. 中国工程物理研究院化工材料研究所, 四川 绵阳 621999)

摘 要: 3,3′-二硝基-4,4′-偶氮呋咱(DAAzF)是3,3′-二氨基-4,4′-氧化偶氮呋咱(DAAF)合成过程的主要杂质之一。目前尚不清楚DAAzF作为杂质对DAAF热性能的影响。为此,本研究使用了基于共溶解-共析出策略的杂质掺杂方法,将0.5%~10% DAAzF均匀掺杂于DAAF中,得到DAAF@DAAzF炸药,并采用同步热分析技术研究了DAAzF对DAAF@DAAzF炸药热性能的影响。结果表明,DAAzF明显降低了DAAF的熔点,10% DAAzF会导致DAAF的熔点从246.4 ℃下降至239.3 ℃。当存在5%的DAAzF时,DAAzF还会与DAAF形成低共熔物。DAAzF的存在会降低DAAF@DAAzF炸药初始热分解过程的活化能和指前因子。总之,DAAzF作为杂质会加速DAAF@DAAzF炸药的热分解,降低其热稳定性。

关键词: DAAF;DAAzF;热性能;DAAF@DAAzF炸药;杂质
中图分类号: TJ55; O64 **文献标志码:** A **DOI:**10.11943/CJEM2022022
(责编:王馨逸)